$ft = 10^{7.6}$ sec, has the expected value for a first-forbidden $2^- \rightarrow 2^+$ β transition.

An estimate of the upper limit of the $\int B_{ij}$ contribution, on the basis of the modified B_{ij} approximation and the measured energy dependence of the β-γ directional correlation, yields $C_A \int B_{ij} < 0.15 |Y_1|$ if $Y' = 0.25$, and $C_A \int B_{ij} < 0.2 |V_0|$, if $y' > 12$.

The small contribution of the $\int B_{ij}$ component to the 1.40-Mev γ transition of Sb^{122} is somewhat surprising in view of the fact that in the β decay of its sister nucleus Sb^{124}, the B_{ij} matrix element represents the main contribution to the nonunique first-forbidden 2.3-Mev and 1.6-Mev β transitions.[10,11,33-35] There is evidence that the large $\int B_{ij}$ contribution to the Sb^{124} β transitions is a result of the j selection rule. One might have expected that the same selection rule effect is also operative in Sb^{122}, which differs by only two neutrons from Sb^{124}.

Au^{198}

The energy dependence of the β-γ directional correlation involving the 0.96-Mev β transition of Au^{198} agrees very well with the predictions of the ξ approximation. The quantity $R(W)$ is independent of the energy W within less than 8% over the energy range from $W = 1.3$ to $W = 2.9$ (Fig. 8). In addition the shape of the 0.96-Mev β spectrum is well represented by the ξ approximation.[36] The good agreement with the ξ approximation is to be expected for Au^{198}, since the parameter ξ for $Z = 80$ ($\xi = 15$) is considerably larger than $W_0 - 1 = 1.9$.

The parameters V_0 and Y_1 are approximately equal in magnitude but of opposite sign in the 0.96-Mev β transition of Au^{198}: $y' = -1.0_{-0.6}{}^{+0.8}$.[26] An analysis of the β-γ directional correlation data on the basis of the modified B_{ij} approximation yields an estimate of the upper limit of the $\int B_{ij}$ contribution to the 0.96 Mev β transition of Au^{198}: $|C_A \int B_{ij}| < 0.1 |Y_1|$.

The small (if any) contribution of the $\int B_{ij}$ matrix element to the 0.96-Mev β transition of Au^{198} is consistent with the ft value, $ft = 10^{7.5}$ sec, of the β transition.

[33] R. M. Steffen, Phys. Rev. (to be published).
[34] P. Alexander and R. M. Steffen, Phys. Rev. (to be published).
[35] H. Paul, Phys. Rev. **121**, 1175 (1961).

ACKNOWLEDGMENTS

The author would like to express his appreciation to the National Science Foundation for their support during part of this work. The author is indebted to Professor K. Alder of the University of Basel (Switzerland), and to Professor H. D. Jensen of the University of Heidelberg for many illuminating discussions. He also wishes to express his thanks to Dr. Deutsch and Dr. Lipkin of the Université de Louvain and to Dr. Daniel of the Max-Planck Institut für Kernphysik (Heidelberg) for communicating their β-γ circular polarization correlation results prior to publication.

[36] A. H. Wapstra, Nuclear Phys. **9**, 519 (1958/59).

PHYSICAL REVIEW VOLUME 123, NUMBER 5 SEPTEMBER 1, 1961

Magnetic Moments of 69-min Ag^{104} and 27-min Ag^{104m}†

O. Ames, A. M. Bernstein, M. H. Brennan,* and D. R. Hamilton
Palmer Physical Laboratory, Princeton University, Princeton, New Jersey
(Received April 21, 1961)

The hyperfine structure separations of 69-min Ag^{104} and of 27-min Ag^{104m} have been measured using the atomic beam magnetic resonance method. The results are: $\Delta\nu_{I=5}$(69-min Ag^{104}) = 33 $500_{-1000}{}^{+2000}$ Mc/sec, $\Delta\nu_{I=2}$(27-min Ag^{104m}) = 35 000±2000 Mc/sec. The sign of the nuclear magnetic dipole moment has been found to be positive for both states, and by use of the Fermi-Segrè formula one obtains $\mu_I(I=5) = +4.0_{-0.1}{}^{+0.2}$ nm, $\mu_I(I=2) = +3.7 \pm 0.2$ nm. Nuclear configurations which give these moments are discussed and we comment on the difference between Ag^{104} which shows a 2^+, 5^+ angular momentum recoupling doublet and Ag^{106} and Ag^{110} which show a 1^+, 6^+ doublet.

I. INTRODUCTION

In a previous paper[1] we described work performed at this laboratory to find the correct assignments of spins, half-lives, and γ rays to the neutron-deficient silver isotopes with mass numbers 102, 103, and 104. The isotope Ag^{104} was studied in the most detail and was found to have a ground state with $I = 5$ and a half-life of 69 min. In addition, Ag^{104} has a low-lying isomeric state with $I = 2$ and a half-life of 27 min.

We have measured the nuclear magnet dipole moment of the $I = 5$ and $I = 2$ states in Ag^{104} by the atomic-beam magnetic-resonance method. The large values of the zero-field hyperfine structure separations made it necessary to perform these measurements by observing multiple-quantum transitions, and made

† This work was supported by the U. S. Atomic Energy Commission and the Higgins Scientific Trust Fund.
* Present address, Department of Physics, University of Sydney, Sydney, Australia.
[1] O. Ames, A. M. Bernstein, M. H. Brennan, R. A. Haberstroh, and D. R. Hamilton, Phys. Rev. **118**, 1599 (1960).

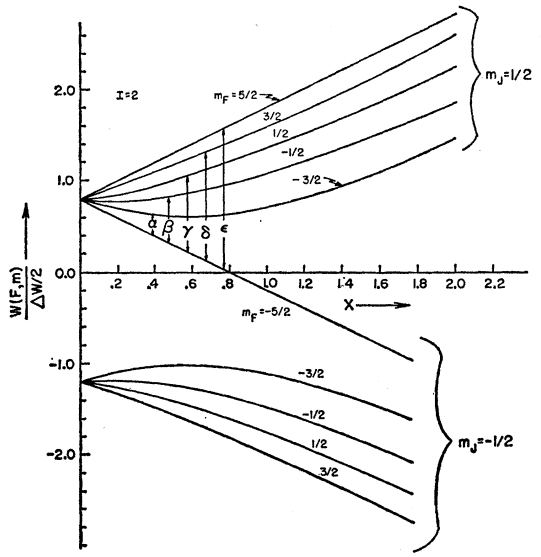

FIG. 1. The energy levels of an atom with $J=1/2$ and $I=2$ in a magnetic field H_0: $x=[(-\mu_J/J+\mu_I/I)/\Delta W]H_0$.

possible a direct determination of the sign of the nuclear moments.

In the next section we describe the theory and discuss the conditions for observing the various resonance transitions. In Sec. III the apparatus is described and in Sec. IV the details of the experiment are presented. The results are shown and discussed in Secs. V and VI.

II. THEORY

The energy levels for an atom with $J=\frac{1}{2}$ in an external magnetic field H_0 are given by the Breit-Rabi formula.[2,3] Figure 1 shows an energy-level diagram for the case that $J=\frac{1}{2}$, $I=2$, and $\mu_I>0$. The quantity $\Delta W/h$ is the hyperfine structure separation $\Delta\nu$ and $x=(-\mu_J/J+\mu_I/I)H_0/\Delta W$. Those $\Delta F=0$ transitions that we can observe in an atomic-beam experiment are indicated by α, $\beta\cdots\epsilon$. The transition usually observed for a measurement of $\Delta\nu$ is the single-quantum transition α. By the dipole selection rules the other transitions can only occur by the emission or absorption of more than one quantum. The transition γ, for example, could occur if the atom emitted 3 quanta each of the appropriate frequency or if the atom emitted 3 quanta at the frequency

$$\nu_{3Q}=[W(\tfrac{1}{2})-W(-\tfrac{5}{2})]/3h.$$

We shall refer to this latter event as a multiple-quantum transition. By expanding the Breit-Rabi formula up to second order in H_0 we can obtain a general formula for the frequency at which a multiple-quantum transition will occur:

$$\nu_{N,m_i}=\left(\frac{g_J}{2}-\frac{\mu_I}{\mu_0}\right)\frac{\mu_0 H_0}{Fh}+\frac{N-2m_i}{4F^2h^2}\frac{(g_J-g_I)^2\mu_0 H_0^2}{\Delta\nu}+\cdots, \quad (1)$$

where $N=$the quantum multiplicity, $m_i=$the magnetic quantum number of the initial state.

For future reference we shall define the quantities ν_l (l for linear) and ν_0:

$$\nu_l=\left(\frac{g_J}{2}-\frac{\mu_I}{\mu_0}\right)\frac{\mu_0 H_0}{Fh}, \quad (2)$$

$$\nu_0=g_J\mu_0 H_0/2Fh. \quad (3)$$

From Eq. (1) we see that if the quadratic term is sufficiently small, in particular, if $2I\nu_0^2/\Delta\nu$ is much less than a linewidth, the frequency associated with the transition α and also with all the multiple-quantum transitions will be given by (2). We note that if g_J is known with sufficient accuracy, a high-resolution measurement of ν_l will yield a value for μ_I. As the static field H_0 is increased the second-order terms become important and the multiple quantum transitions will be separated by (neglecting terms in g_I)

$$\delta\nu=\nu_0^2/\Delta\nu. \quad (4)$$

Thus a measure of the frequency spacing between the multiple-quantum transitions will yield a value for the hyperfine structure separation $\Delta\nu$. The value of $\Delta\nu$ can also be obtained by measuring the shift of the 1 quantum transition frequency from ν_l. A knowledge of $\Delta\nu$

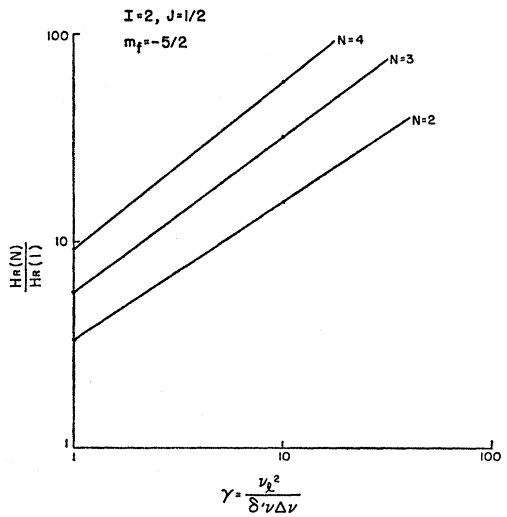

FIG. 2. Ratio of the optimum field, $H_R(N)$, for an N-quantum transition to the optimum field for a single-quantum transition.

[2] G. Breit and I. I. Rabi, Phys. Rev. 38, 2082 (1931).
[3] N. F. Ramsey, *Molecular Beams* (Oxford University Press, New York, 1956).

enables one to obtain the magnitude of μ_I from the Fermi-Segrè formula.[3]

We discuss next the magnitude of the radio-frequency field H_R necessary to induce multiple-quantum transitions. Ramsey[3] has treated in detail the problem of the rf field magnitude necessary to saturate the single-quantum transition. Hack[4] has considered the general problem, and we can summarize by saying that the more the intermediate states deviate from equally spaced levels between the initial and final states, the larger is the field H_R needed to saturate the transition. Christensen *et al.*[5] have compared Hack's theory with experiment in the case of K^{39} and have obtained good agreement.

For the case of $J=\frac{1}{2}$ and $I=2$ the theory gives the curves of Fig. 2. The ratio of the optimum N-quantum field to the optimum 1-quantum field is plotted as a function of the dimensionless parameter $\gamma=\nu_1^2/(\delta'\nu\Delta\nu)$, where $\delta'\nu$ is the natural linewidth of the resonance, and can be found from the time that the atom spends in the perturbing field H_R. It should be pointed out that the multiple-quantum theory as developed by Hack[4] is valid in the case that $\gamma>1$; that is, where the multiple-quantum peaks are separated by more than the uncertainty width $\delta'\nu$.

III. APPARATUS

The focusing atomic-beam apparatus built by Lemonick, Pipkin, and Hamilton,[6] and modified as described below was used for the determination of the hfs separations. Figure 3 shows the position of the oven, the magnets, stops, and the detector system. Note that the vertical and horizontal dimensions are drawn to different scales. The collector for radioactive atoms is built in two pieces, a center button 0.6 in. in diameter and a concentric disk 2 in. in diameter. These are fastened together and are inserted into the apparatus through an air lock, the axis of the button-disk system coinciding with the axis of the apparatus. A typical pair of orbits is shown in Fig. 3. Atoms entering the A magnet such that $\partial W/\partial x>0$ (see Fig. 1) seek the axis of the machine, and if no transition occurs in the C-field region they also seek the axis in the B field and will strike the center button. The dashed line shows the trajectory of an atom which has undergone an appropriate transition in the C field and thus enters the B field with $\partial W/\partial x<0$; this atom will seek regions of strong magnetic field, and upon leaving the magnet will strike the outer disk. The button and disk are removed from the apparatus after an exposure and are counted in separate counters. In the case that no transition occurs most of the atoms will strike the button, but some will still strike the disk because of scattering and

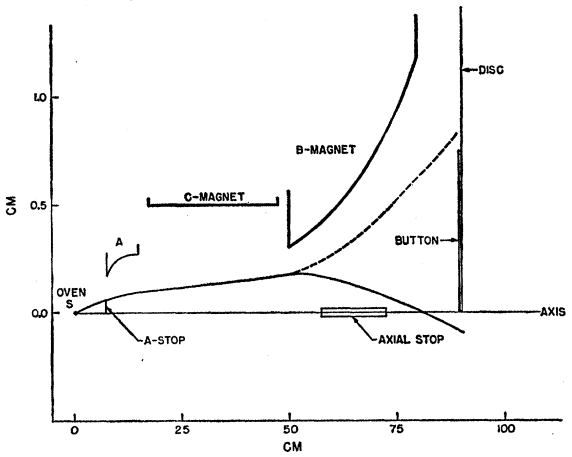

FIG. 3. Cross-sectional plan of the apparatus. Notice that the horizontal and vertical scales are different. The dashed line indicates the trajectory of an atom that has undergone a transition in the C field.

Majorana transitions.[3] The sum of the count rates on the button and on the disk gives a measure of the total beam while the ratio of the disk count rate to the button count rate D/B will indicate the presence of a resonance transition. For the case that no resonance occurs D/B is about 0.025 for silver. On resonance this may increase to 0.050 or higher. The major advantage of this detection system is that it allows one to make measurements using beams that cannot be maintained constant in time. The ratio D/B is essentially independent of $D+B$. This feature was found to be essential for these measurements.

If the atoms emerging from the oven were all of the same velocity it would be possible to image the oven orifice at the detector position. The distribution in atom velocities makes this impossible and results in the "focused" beam having a considerable spread. The axial B-magnet stop was inserted to prevent the low-velocity atoms from crossing the axis in the B magnet, thus reducing the spread of unflopped atoms on the detector plane. This, together with the choice of an 0.6-in. diameter center button, gave a relatively high D/B ratio at resonance while maintaining high count rates.

IV. EXPERIMENT

The radioactive silver was produced by bombarding a 0.016-in. thick stack of natural Pd foils in the 18.5-Mev proton beam of the Princeton cyclotron. Bombardments of about 1 hr with an internal beam current of approximately 0.5 μa produced sufficient activity for measurements on either state. After bombardment the Pd foils were removed from the cyclotron and placed in a small molybdenum oven which was then inserted into the oven chamber of the beams apparatus. For work on the 27-min level the oven was inserted through an air lock which is now an integral part of the appa-

[4] M. N. Hack, Phys. Rev. **104**, 84 (1956).
[5] R. L. Christensen, D. R. Hamilton, H. G. Bennewitz, J. B. Reynolds, and H. H. Stroke, Phys. Rev. **122**, 1302 (1961).
[6] A. Lemonick, F. M. Pipkin, and D. R. Hamilton, Rev. Sci. Instr. **26**, 1112 (1955).

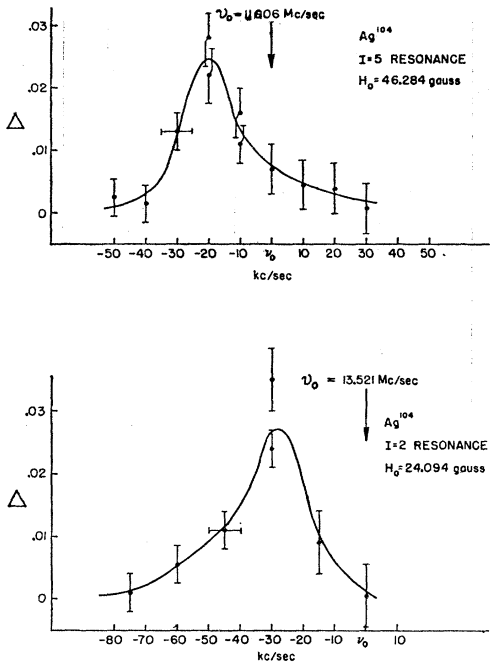

FIG. 4. The $I=5$ and $I=2$ resonance patterns at 46 and 24 gauss, respectively. Δ is the D/B ratio with the rf on minus the D/B ratio with the rf off.

ratus. This meant that a beam could be obtained within 10 min of removal from the cyclotron. Well-behaved silver beams were obtained by heating the oven to a temperature ≈1500°C (optical pyrometer temperature ≈1300°C). By slowly raising the temperature throughout the run, it was possible to keep the beam intensity fairly constant despite radioactive decay and depletion of Ag in the oven. Starting at a temperature much higher than 1500°C, or running the temperature too high during a run, resulted in marked instabilities in the D/B ratio. It was observed that at the end of a run the palladium foils had not quite melted. The instabilities in the D/B ratio and in the general behavior of the beam were apparently associated with the complete melting of the Pd.

The buttons and disks used for collecting the beam were made of copper and were carefully cleaned by rubbing with steel wool and soaking in acetone and then alcohol immediately before the run. The counters used are described in a previous paper.[1] Exposure times varied from 3 to 5 min, and about 1 min was required from the time a collector was removed until exposure could start on the next collector. The beam generally held up long enough to expose from 7 to 10 collectors. In the case that 10 collectors were exposed, the first, fourth, seventh, and tenth were taken with the rf turned off in order to give a measure of the background. Typical count rates with the rf off were about 4000 counts per minute on the button and 100 counts per minute on the disk, giving a D/B ratio of 0.025. This ratio might increase to 0.050 on a resonance. Runs in which the no rf D/B ratio varied largely were rejected.

The C magnet was powered by two 6-v storage batteries and the current through the magnet was monitored using a Leeds and Northrup potentiometer. The C field was calibrated using a beam of K^{39} and was generally measured immediately before and just after a radioactive run. Small drifts that occurred during the course of the run could generally be correlated with the potentiometer readings.

Several different oscillators were used for producing the field H_R; Rohde and Schwarz types SMLR and SMLM, a Hewlett-Packard 608A, and a homemade Clapp oscillator. At high values of the field H_0, some of the multiple-quantum resonances in silver required more rf power than could be supplied by these oscillators. In these instances the rf was amplified by a James Millen Company push-pull power amplifier. The signal picked up by a small loop concentric with the radio-frequency loop was rectified by a diode and used as a monitor of the field strength H_R. The frequency was measured by a Hewlett-Packard 524-B electronic counter.

V. RESULTS

Figure 4 shows the $I=5$ and $I=2$ resonances at 46 and 24 gauss, respectively. The quantity Δ is the D/B ratio with the rf on minus the D/B ratio with the rf off. At these values of H_0, and for all lower values, the resonance pattern shows a single peak and no structure is discernible. We note, however, that the resonances occur below the frequency ν_0, the frequency at which a resonance would occur if the nuclear moment were

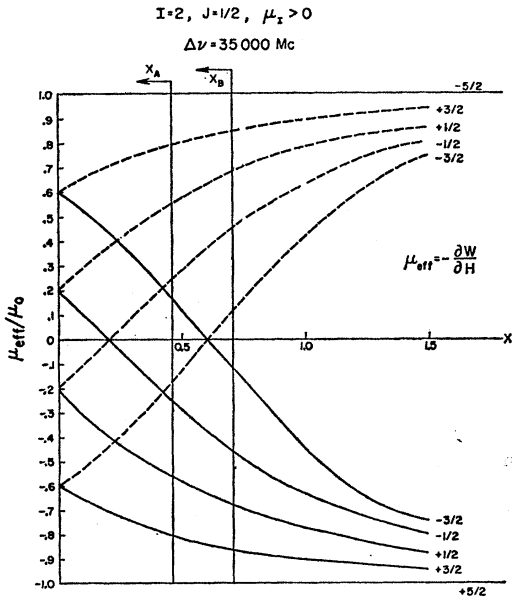

FIG. 5. An effective-moment diagram for $J=1/2$, $I=2$, $\mu_I>0$, and $\Delta\nu=35\,000$ Mc/sec. $\mu_{eff}=-\partial W/\partial H$ (see Fig. 1). x_A and x_B correspond to the values at or near the pole tips of the A and B magnets, respectively.

zero. A shift of the resonance pattern to frequencies higher than ν_0 might be explained by the presence of the quadratic term in Eq. (1). The shift to lower frequencies can only occur if $\mu_I>0$. From these data then we infer that the nuclear magnetic dipole moments of the $I=5$ and $I=2$ states in Ag^{104} are both positive. The magnitude of the shift further suggests that the moments are large and equivalently that $\Delta\nu$, the zero-field hyperfine structure separation, is of the order of 40 000 Mc/sec for both states. This high value for $\Delta\nu$ has some interesting consequences which were first observed by Christensen *et al.*[7] in measurements on Au^{198}. We shall discuss this briefly.

In Fig. 5 we have plotted μ_{eff}/μ_0 vs x for $I=2$ where $\mu_{\text{eff}}=-\partial W/\partial H$ and x is defined above. The solid lines refer to the states where $F=I+\frac{1}{2}$, the dotted lines to the states of $F=I-\frac{1}{2}$. Taking the value of $\Delta\nu$ for the $I=2$ state as 35 000 Mc/sec, and using the results of early magnetic-field measurements on the apparatus,[8] we compute the values of x at or near the pole tips of the A and B magnets. These are denoted by x_A and x_B, respectively. The condition that an atom seek the axis of the apparatus is then that $\mu_{\text{eff}}/\mu_0<0$. It is quite clear from Fig. 5 that for the large $\Delta\nu$ and consequently small value of x_A, the state $m_F=-\frac{3}{2}$ is not focused by the A magnet and therefore cannot be an initial state. Thus the transition α of Fig. 1 cannot be observed. The transitions β, γ, δ, and ϵ should, however, be observable, and we might expect to see some transitions for which the state $m_F=-\frac{3}{2}$ is a final state. Another set of transitions that might be observed in this case are in the $F=I-\frac{1}{2}$ set of levels where $m_F=-\frac{3}{2}$ is a possible initial state. These transitions were not looked for in the experiments.

For those values of the field H_0 for which the quadratic term in Eq. (1) is no longer negligible the resonance pattern will be split into separate peaks, one for each value of $N-2m_i$ which quantity we shall refer to as P. In Fig. 6 we indicate the correspondence between m_i, m_f, N, and the P values which are enclosed in the boxes.

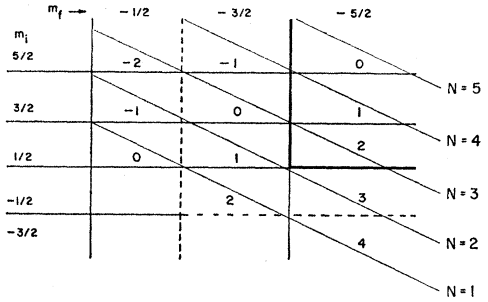

FIG. 6. Relationships between m_i, m_f, P, and N.

From the magnitudes of the μ_{eff}/μ_0 values for each transition we can make qualitative predictions about the relative sizes of the resonances (see Fig. 5). In Fig. 6 the resonances that should be strong are enclosed in the solid line, while the weaker ones are enclosed by the dashed line. No resonances outside the dashed line are expected to be visible. A similar table can be constructed for the case that $I=5$. These qualitative predictions are borne out by the experimental data.

We shall now discuss the data obtained at higher values of the C field.

$I=5$

At a field of 200 gauss the $I=5$ pattern showed well-resolved peaks and the data are shown in Fig. 7. The upper arrows indicate the resonance positions used in the analysis. We shall discuss below the method of assigning the various P values to the resonances.

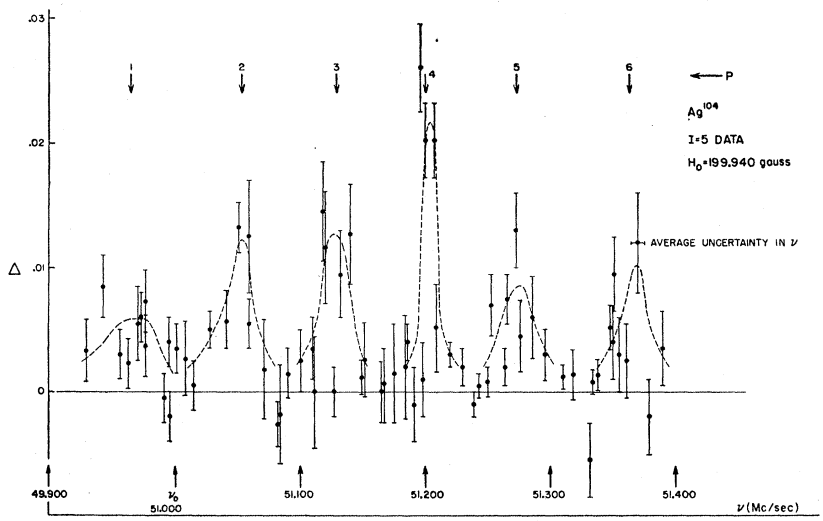

FIG. 7. The $I=5$ data at $H_0=200$ gauss. The arrows under the values of P indicate the resonance positions used in the analysis.

[7] R. L. Christensen, D. R. Hamilton, A. Lemonick, F. M. Pipkin, J. B. Reynolds, and H. H. Stroke, Phys. Rev. **101**, 1389 (1956).
[8] A. Lemonick, F. M. Pipkin, and D. R. Hamilton (private communication).

TABLE I. Summary of experimental data.

I	H_0 (gauss)	ν_0 (Mc/sec)	P	N	$\nu-\nu_0$ (on resonance) (kc/sec)	$H_R/H_R(1)$	Opt. for N
2	24.1	13.5	not resolved		-30 ± 10	from 2.5 to 5.6	···
5	46.3	11.8	not resolved		-20 ± 7	≈ 6	···
5	200	5	1	10, 8, (6)	-35 ± 15		
			2	9, 7, (5)	$+54\pm 8$		
			3	8, 6, (4)	$+129\pm 9$	≈ 48	6
			4	7, 5, (3)	$+201\pm 7$		
			5	6, 4, (2)	$+273\pm12$		
			6	5, 3	$+363\pm12$		
2	90.9	51	-1	4	-177 ± 13	43	5 or >5
			0	5, 3	-97 ± 9	43	5 or >5
			1	4, 2	-31 ± 9	15, 43	3–4, 5 or >5
			2 not clear	3, 1	$0\rightarrow+55$	15, 43	3–4, 5 or >5
			3	2	$+134\pm21$	15	3–4
2	124.7	70	0	5, 3	-131 ± 19	74	5 or >5
			1	4, 2	-14 ± 15	↓	↓
			2	3, 1	between $+80$ and $+150$		

The uncertainty in the frequency arose from two sources; firstly, from uncertainties in calibrating the C field using the beam of K^{39}, and secondly, from drifts in the C field in the course of a radioactive run. In no cases did the combination of these effects result in an uncertainty exceeding ±10 kc/sec.

The vertical errors are due completely to statistics. Since Δ is the D/B ratio with rf on less the value with rf off, the error bars result from the statistical uncertainty in both measurements in addition to that added in determining the counter background. It is also quite possible that two separate runs covering the same frequencies will show varying peak intensities because of slight differences in the positioning of the oven.

A possible systematic source of error concerns the amount of radio-frequency power used to induce a transition. The theory as developed by Hack[4] and Salwen[9] predicts energy level shifts as the rf power is increased by a large amount over that necessary for saturation and also predicts changes in the resonance width. Kusch[10] studied these effects in detail using a beam of K^{39} and found agreement with theory as long as the rf field was not made too large. The discrepancies at high values of H_R were presumably explainable in terms of the spatial distribution of the radio-frequency field. Experiments in this laboratory using beams of K^{39} showed large shifts in the resonance position if the field H_R was increased far above the value required for maximum transition probability.[11] Because of the simple loop used in these experiments the shifts probably arose from the extension of the rf field into regions of C-magnet inhomogeneity. Because of these effects considerable care was exercised in taking the Ag data to have the magnitude of the radio-frequency field roughly appropriate to the multiplicity of the transitions being observed. In Table I we list the values of the fields used, H_R, as compared to those necessary to saturate the single-quantum resonance, $H_R(1)$. The right-hand column indicates the multiplicities for which the values of H_R are optimum.

Combining Eqs. (1) through (4), and recalling the definition of the integer P, we see that

$$\nu-\nu_l=P\delta\nu, \tag{5}$$

where ν is the frequency at which a resonance occurs.

This equation is exact to second order in H_0. For the $I=5$ state at 200 gauss the cubic term will give rise to shifts of less than 0.5 kc/sec, so that (5) is a good approximation and we should expect the resonances to be equally spaced.

Thus, in Fig. 8, we have plotted the resonance positions relative to ν_0 as a function of ordinal numbers. The vertical error bars represent the largest reasonable range over which the resonances could be interpreted as occurring. The best straight-line fit to the six points corresponds to a peak spacing of 77.8 kc/sec. From this value of $\delta\nu$ and using Eq. (4), we compute that $\Delta\nu=33\,500$ Mc/sec, and from the Fermi-Segrè formula using the mean of the values of μ_I and $\Delta\nu$ obtained for Ag^{107} and Ag^{109},[12] we get $\mu_I=4.0$ nuclear magnetons. Inserting this value for the moment into the linear term in Eq. (1) we find that ν_l falls 111 kc/sec below ν_0. If the data are internally consistent the line corresponding to $\delta\nu=77.8$ kc/sec should cross $\nu-\nu_0=-111$ kc/sec at one of the ordinals, in particular the one which we can now label as $P=0$. In this case the consistency is very good. The dashed lines corresponding to $\delta\nu=79.4$ and 73.6 kc/sec show the limits of

[9] H. Salwen, Phys. Rev. **101**, 623 (1956).
[10] P. Kusch, Phys. Rev. **101**, 627 (1956).
[11] W. J. Kossler (private communication).
[12] P. Kusch and V. W. Hughes, *Handbuch der Physik*, edited by S. Flügge (Springer-Verlag, Berlin, 1959), Vol. 37, Part 1.

uncertainty, and the values of $\nu_l-\nu_0$ derived from these numbers are indicated by the circles. The value for g_J of silver used for this analysis was $g_J=2.002320 \pm 0.000105$.[12] A more accurate value has recently been obtained, $g_J=2.002333\pm0.000010$.[13] The difference is of no significance to this analysis.

The data are summarized in Table I. The values of N associated with the various P values were determined in a manner similar to that used for $I=2$ (see Fig. 6).

Summarizing the results for the $I=5$, 69-min ground state of Ag^{104},

$$\Delta\nu=33\ 500_{-1000}{}^{+2000}\ \text{Mc/sec},$$

and

$$\mu_I=+4.0_{-0.1}{}^{+0.2}\ \text{nm}.$$

$I=2$

The high-field $I=2$ runs were made at 90.9 and 124.7 gauss and the results are summarized in Table I. At both of these fields the resonances were resolved and the results were in good qualitative agreement with those predicted in Fig. 6. The resonance $P=-1$ corresponding to the transition $m_i=\frac{5}{2}\rightarrow m_f=-\frac{3}{2}$ was observed and was weak as expected. The method of analysis was identical to that used for the $I=5$ state and, as in that case, the terms in $H_0{}^3$ could be neglected.

The best fit to the data gave for the $I=2$, 27-min isomeric state in Ag^{104}

$$\Delta\nu=35\ 000\pm2000\ \text{Mc/sec},\quad \mu_I=+3.7\pm0.2\ \text{nm}.$$

VI. DISCUSSION

The known energy levels of the Ag isotopes are shown in Fig. 9. Between 38 and 50 particles, the shell model predicts close competition between the $p_{1/2}$ and $g_{9/2}$ orbitals. For the odd-even Ag isotopes Ag^{105} through Ag^{111}, the $p_{1/2}$ state is the lowest with a $\frac{7}{2}^+$ state [interpreted as $(g_{9/2}{}^7)_{7/2}$] in close competition. (For Ag^{105} the position of the $\frac{7}{2}^+$ level is not known, the 25-kev level not being well established.) For Ag^{103} the $\frac{7}{2}^+$ state is the only known state, and is presumably the ground state. The $\frac{9}{2}^+$ level has been found only in Ag^{109}.

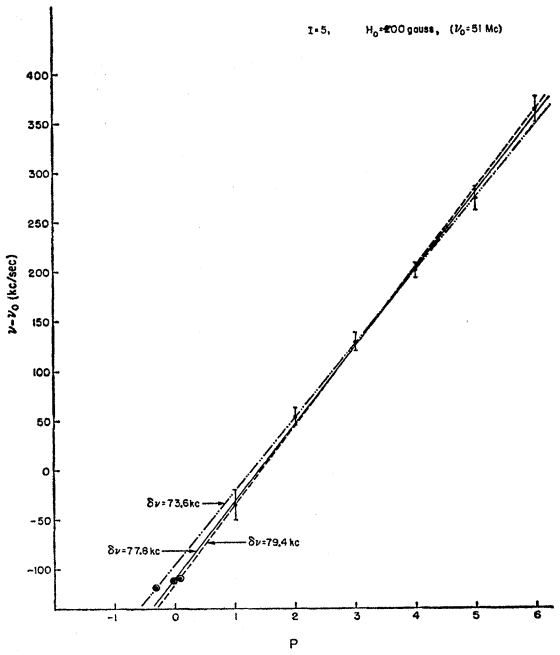

FIG. 8. The position of the resonances observed for $I=5$ at 200 gauss as a function of P. $\delta\nu=77.8$ kc/sec indicates the best fit to the experimental data. The other lines indicate the limits of uncertainty.

The adjacent odd neutron nuclei are, according to the shell model, filling the $g_{7/2}$ and $d_{5/2}$ shells. According to the available data, these nuclei show $\frac{5}{2}^+$ ground states for N between 51 and 63, indicating that in the odd-odd Ag nuclei the neutron configuration appears to be $d_{5/2}{}^{-1}$, with the $g_{7/2}$ neutrons filling in pairs.

From the results of a recent survey of the properties of odd-odd nuclei[14] we can conclude that one might expect the wave function of the odd-odd Ag nuclei to

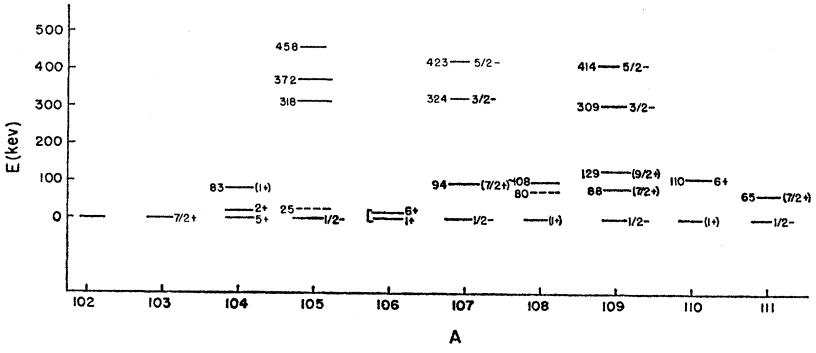

FIG. 9. A summary of the known energy levels in some of the silver isotopes.

[13] G. S. Hayne and H. G. Robinson, Bull. Am. Phys. Soc. **5**, 411 (1960).
[14] M. H. Brennan and A. M. Bernstein, Phys. Rev. **120**, 927 (1960).

TABLE II. Comparison of calculated and experimental moments.

Configuration		$Ag^{104}(I=2)$; $\mu=+3.7\pm0.2$		$Ag^{104}(I=5)$; $\mu=+4.0_{-0.1}^{+02}$.	
Protons	Neutrons	μ_{emp}	μ_s	μ_{emp}	μ_s
$(g_{9/2}^{-3})_{7/2}$	$(d_{5/2}^{-1})$	2.7	3.4	3.4	3.2
$(g_{9/2}^{-3})$	$(d_{5/2}^{-1})$	5.0	6.8	4.5	4.9
$(p_{1/2}^{1})$	$(d_{5/2}^{-1})$	−0.5	−1.6	...	...

have one of the following forms:

(1) $\pi(p_{1/2})$ $\nu(d_{5/2}^{-1})$ $I=2^-$,

(2) $\pi(g_{9/2}^{-3})_{7/2}$ $\nu(d_{5/2}^{-1})$ $I=1^+$ and 6^+ in close competition,

(3) $\pi(g_{9/2}^{-3})_{9/2}$ $\nu(d_{5/2}^{-1})$ $I=2^+$ and 7^+ in close competition.

By $\pi\nu$ we indicate a product wave function of experimentally observed proton and neutron states in the neighboring odd-even nuclei, vector coupled to total spin I. We note that the doublets in (2) and (3) are due to the angular momentum recoupling of single neutron-proton configurations and not to the excitation of single-particle states which is the cause of isomerism in Ag^{107} and Ag^{109}.

In Ag^{106} and Ag^{110} we find the closely spaced 1^+, 6^+ doublet. In Ag^{108} an isomer has been found which may be of this type, but more data are required. Therefore, it seems that (2) is the wave function. However, in Ag^{104} we have a 2^+, 5^+ doublet which does not fit into any of the patterns.

From the product form of the wave function the magnetic moment is given by[15]

$$\mu_I=\tfrac{1}{2}I(g_n+g_p)+\frac{(g_n-g_p)[I_n(I_n+1)-I_p(I_p+1)]}{2(I+1)}.$$

[15] J. P. Elliott and A. M. Lane, *Handbuch der Physik*, edited by S. Flügge (Springer-Verlag, Berlin, 1957), Vol. 39, p. 298.

We can use either Schmidt or experimental moments for the g factor of the odd groups to determine $\mu_{Schmidt}$ or μ_{emp}. The use of experimental g factors from neighboring odd-even nuclei takes into account configuration mixing and possible g-factor quenching in the odd-A nuclei. Using these,[16] we obtain the values for μ_I listed in Table II, from which we observe that the moments for both the $I=2$ and $I=5$ states lie approximately halfway between the value of μ_{emp} calculated for the $\frac{7}{2}^+$ and $\frac{9}{2}^+$ proton states coupled to the $\frac{5}{2}^+$ neutron state. We note that even with "relatively pure" configurations μ_{emp} usually cannot be expected to agree with the experimental moment to closer than approximately 0.2 nuclear magneton.[14] On the basis of the moment it appears that the 2^+, 5^+ doublet can be written in the form:

$$\psi(Ag^{104})\approx\frac{1}{\sqrt{2}}[\pi(g_{9/2}^{-3})_{7/2}\nu(d_{5/2}^{-1})+\pi(g_{9/2}^{-3})_{9/2}\nu(d_{5/2}^{-1})],$$

and that for Ag^{106} and Ag^{110} (and perhaps Ag^{108})

$$\psi(Ag^{106})\approx\pi(g_{9/2}^{-3})_{7/2}\nu(d_{5/2}^{-1}).$$

Why this change should occur between Ag^{106} and Ag^{104} is not clear. Perhaps the data on the $\frac{9}{2}^+$ and $\frac{7}{2}^+$ levels in Ag^{103} and Ag^{105} would shed some light on this. Also, the measurement of the moments in Ag^{106} and Ag^{110} would test the form of the proposed wave function.

Preliminary measurements at this laboratory on the $I=1$ state in Ag^{106} indicate that the magnetic moment is large and positive.

ACKNOWLEDGMENTS

We are indebted to J. C. Walker, D. L. Harris, and W. J. Kossler for assistance in taking data.

[16] For the $g_{9/2}$ protons, Tc^{99}, In^{113}, and In^{115} were used, and for the $d_{5/2}$ neutrons, Ru^{99}, Ru^{101}, and Pd^{105}. The $p_{1/2}$ proton g_{emp} was obtained by considering Ag^{105}, Ag^{107}, and Ag^{109}, as well as Rh^{103}.